

† Electronic Supplementary Information (ESI)

Computational study of Interactions of Anti-cancer drug Eribulin with Human Tubulin Isoforms†

Khushnandan Rai^a, Bajarang Vasant Kumbhar^{a,b}, Dulal Panda^a, and Ambarish Kunwar^{a†}

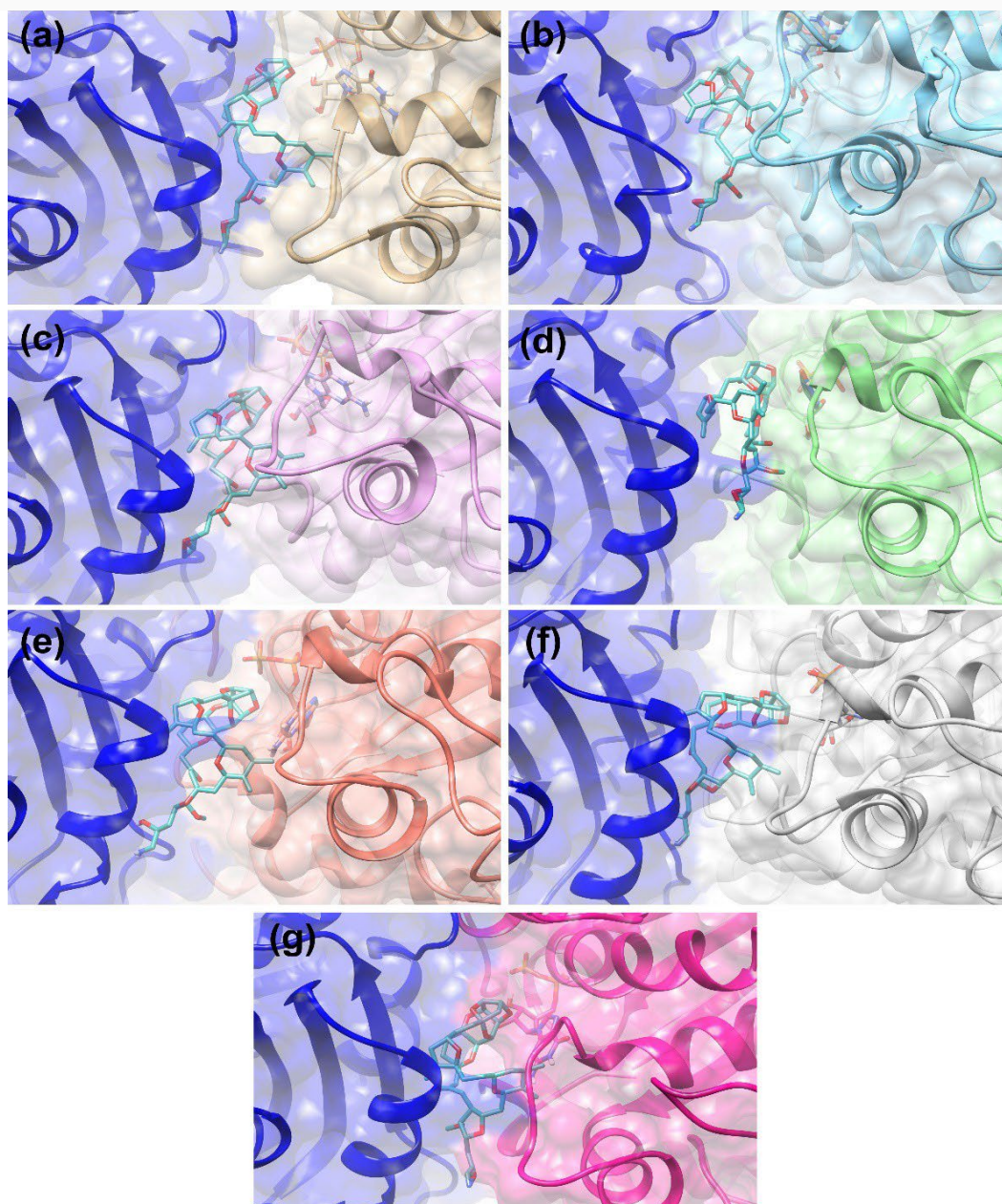


Fig. S1: 3D conformation of average structure of eribulin obtained from last 10 ns of equilibrium state for combination of α_1 (blue) with (a) β_1 (golden), (b) β_{II} (cyan), (c) β_{III} (hot pink), (d) β_{IV} (green), (e) β_{VI} (orange), (f) β_{VII} (light gray), (g) β_{VIII} (magenta).

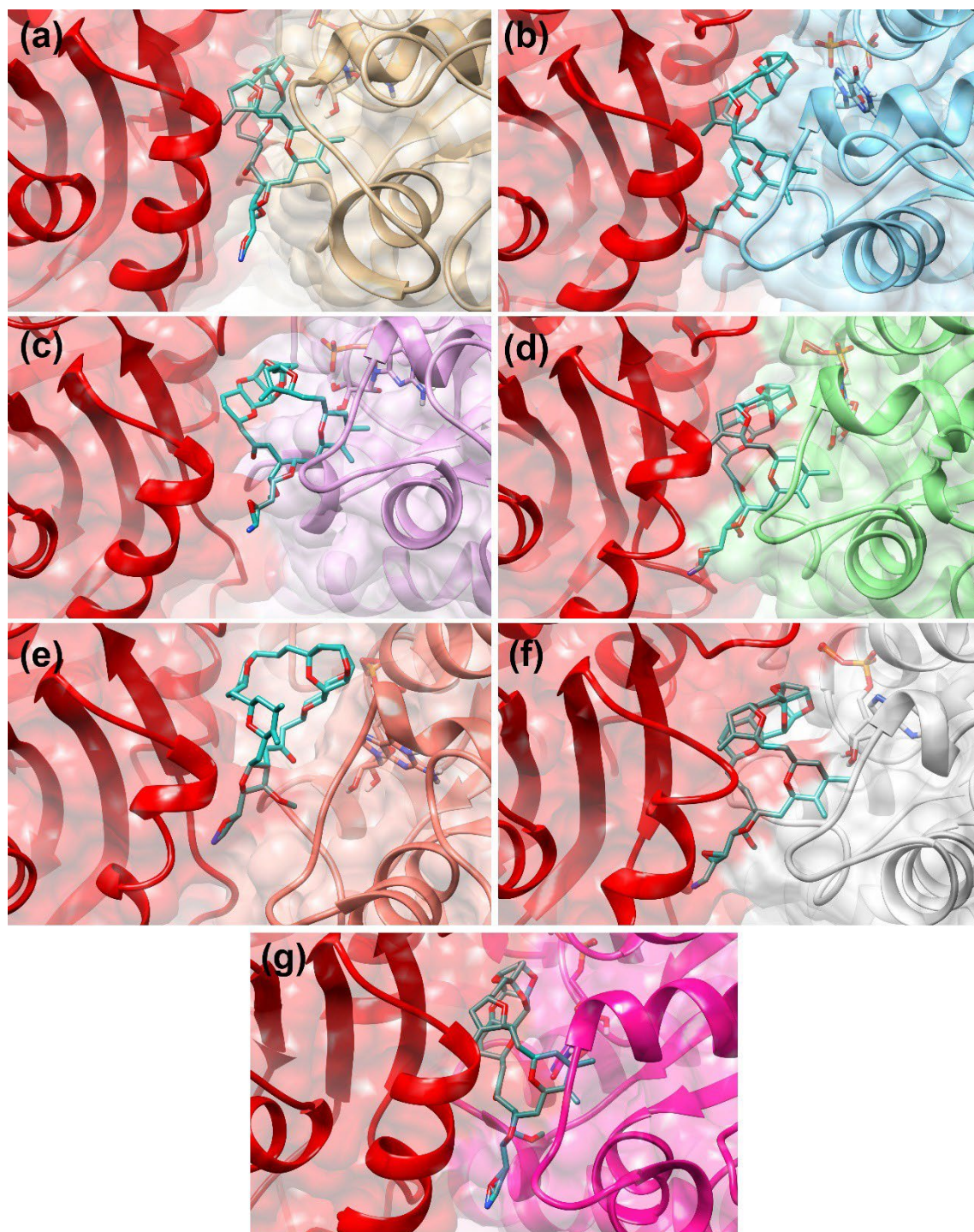


Fig. S2: 3D conformation of average structure of eribulin obtained from last 10 ns of equilibrium state for combination of α _{VIII} (red) with (a) β _I (golden), (b) β _{II} (cyan), (c) β _{III} (hot pink), (d) β _{IV} (green), (e) β _{VI} (orange), (f) β _{VII} (light gray), (g) β _{VIII} (magenta).

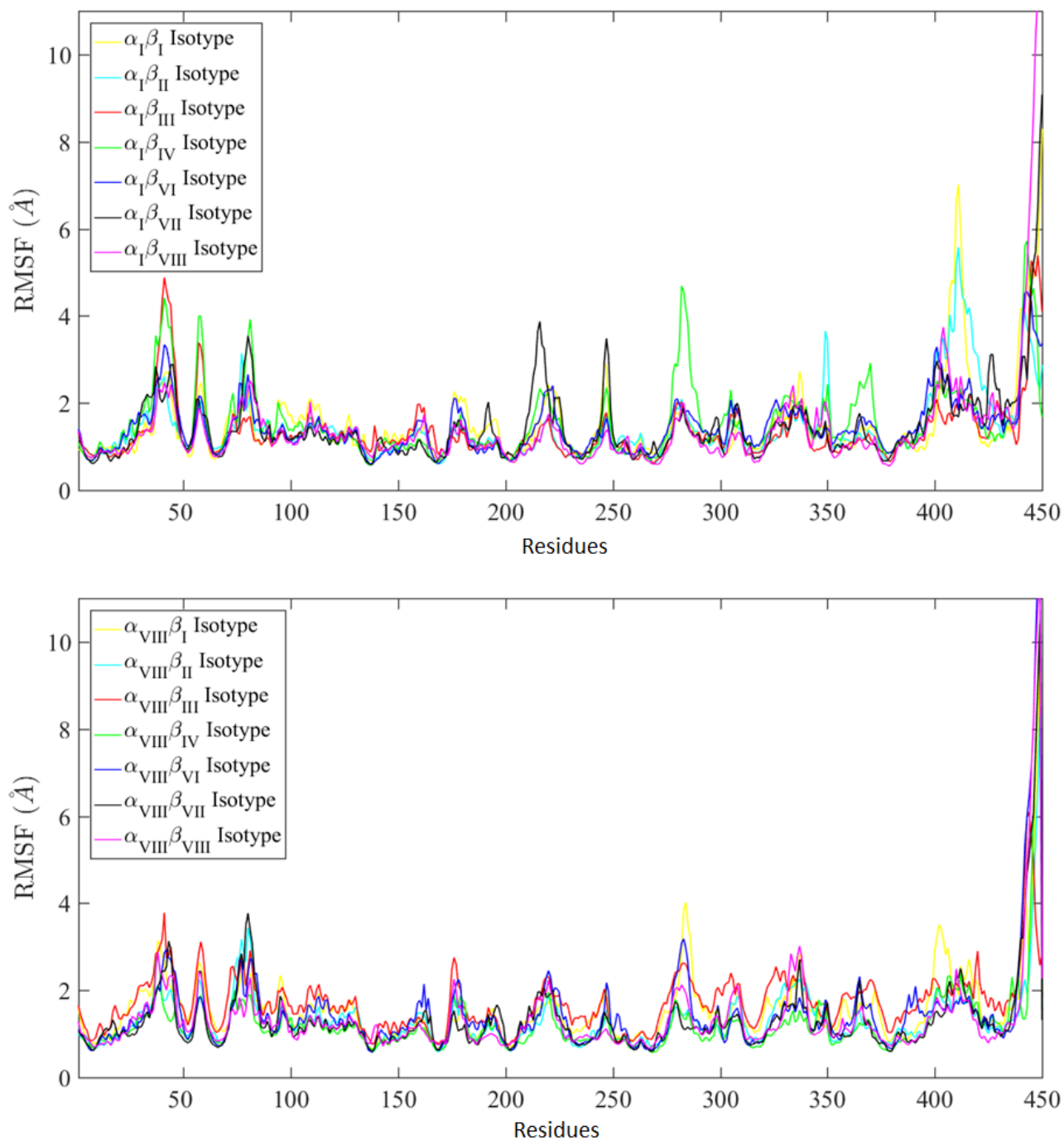


Fig. S3: Root mean square fluctuations (RMSF) of α -tubulin for combination of α_I with 7 β tubulin isotypes (upper), and combination of α_{VIII} with 7 β tubulin isotypes (lower).

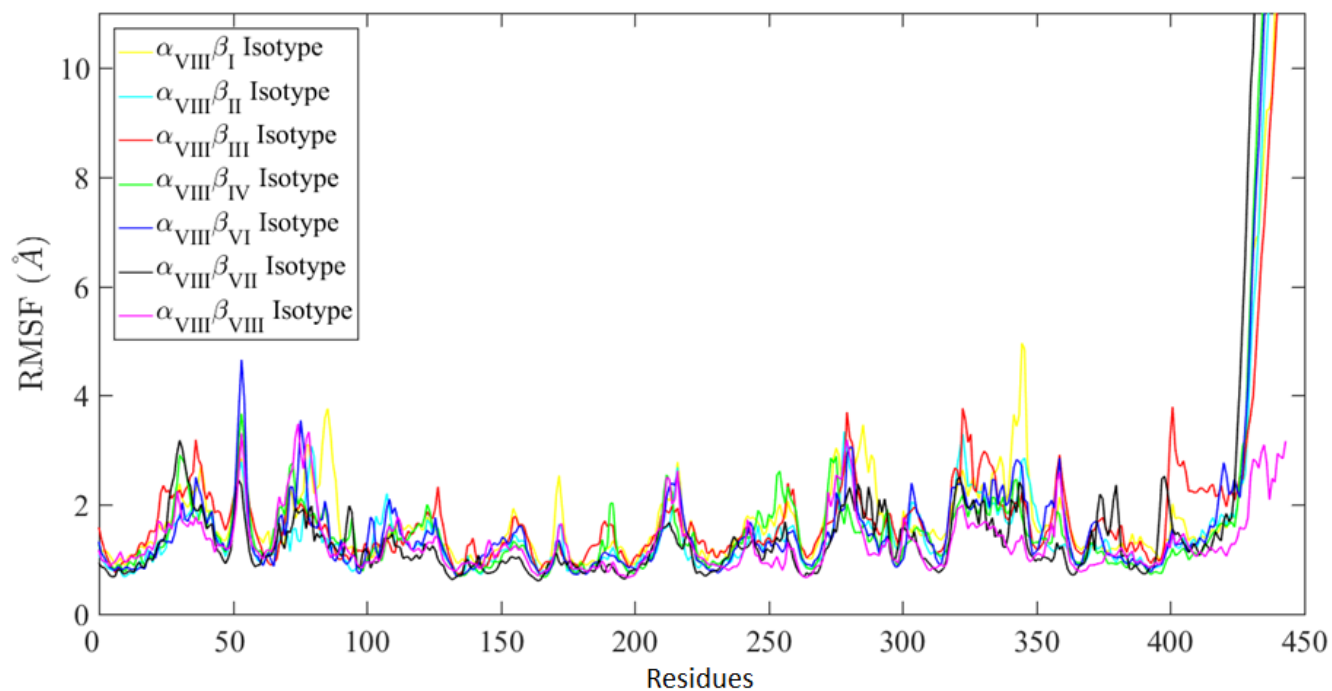
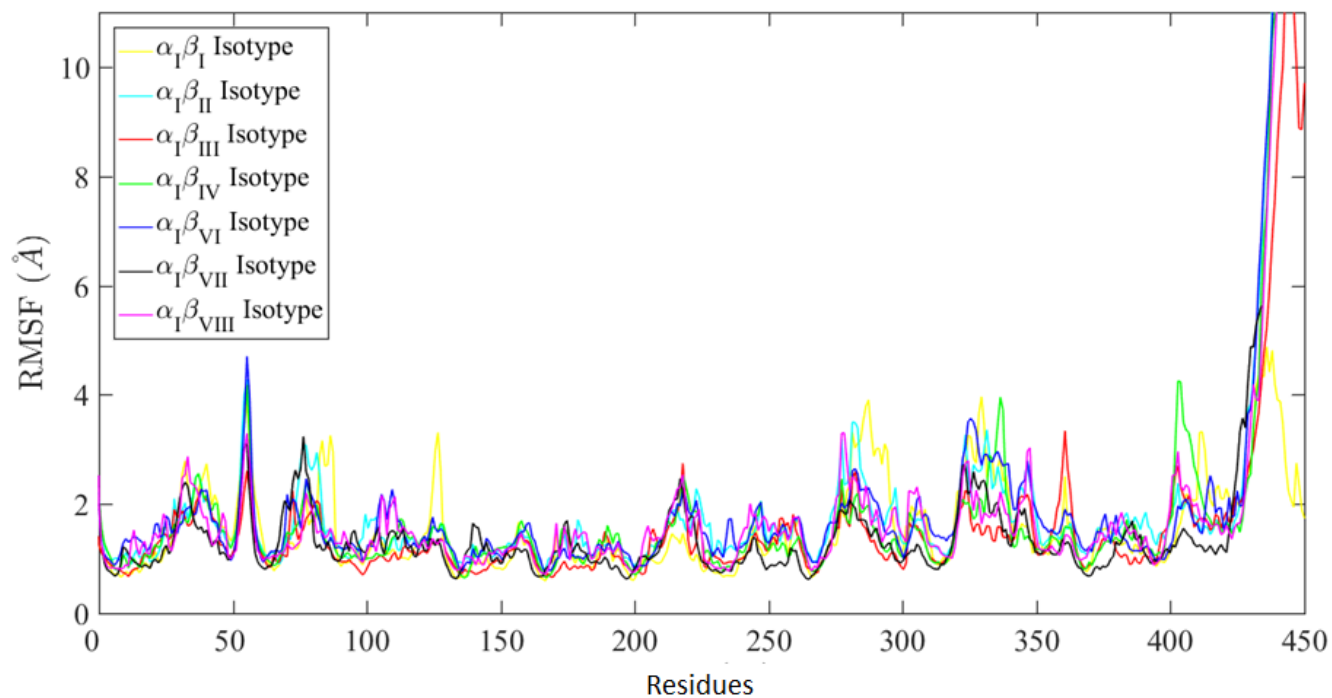


Fig. S4: Root mean square fluctuations (RMSF) of β -tubulin for combination of α_I with 7 β tubulin isotypes (upper), and combination of α_{VIII} with 7 β tubulin isotypes (lower).

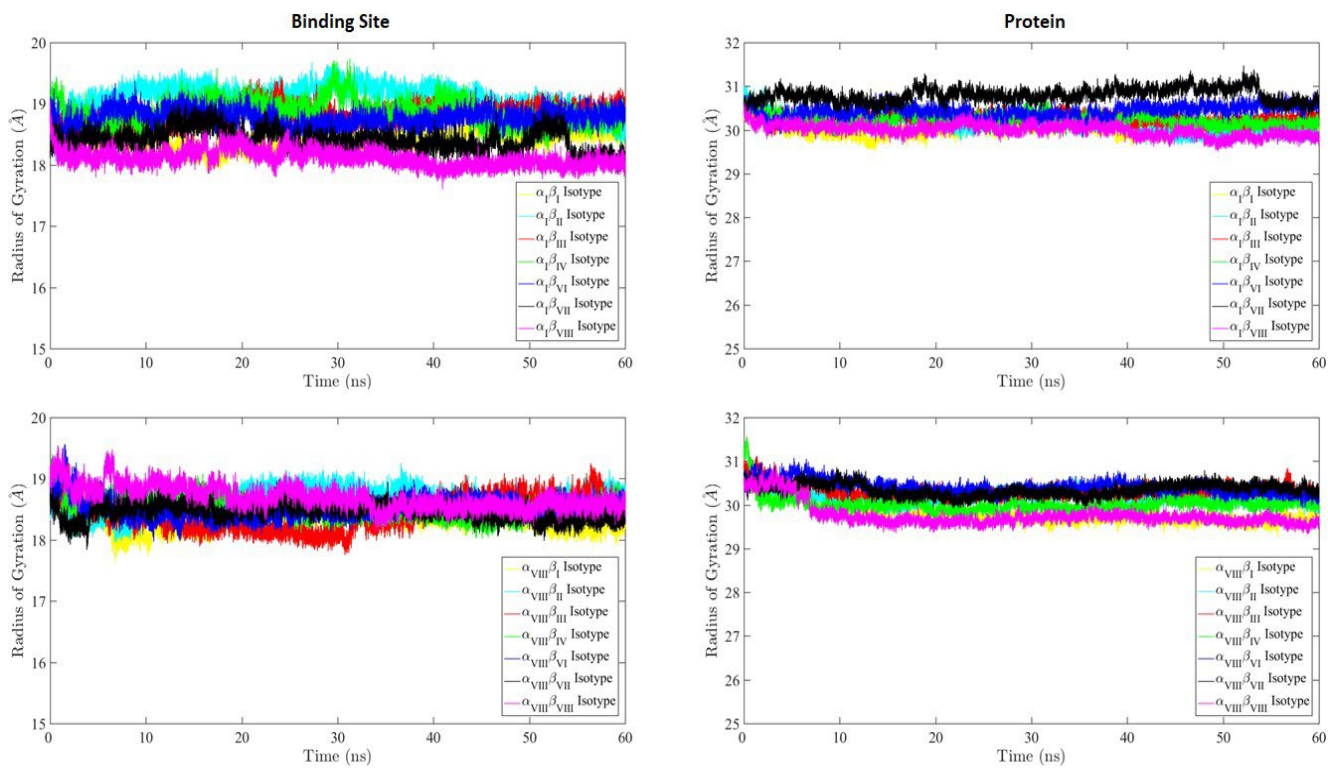


Fig. S5: Radius of gyration of binding site (left) and entire protein (right) during MD simulations for α_I (upper) and α_{VIII} (lower) with all β tubulins isotypes.

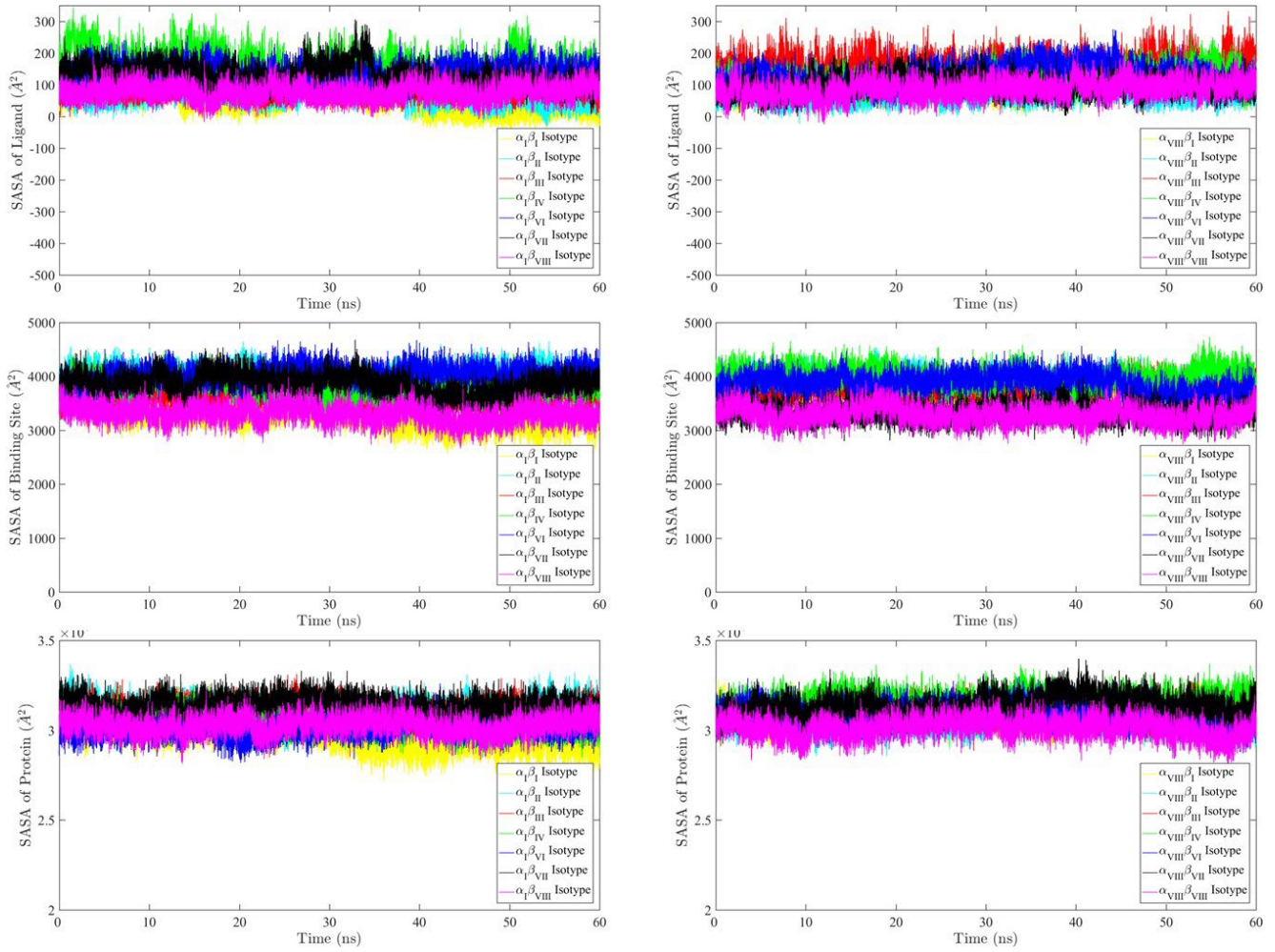


Fig. S6: Solvent accessible surface area (SASA) of ligand (upper), binding site (middle) and protein (lower) for all tubulin isotypes combinations (α_i (left) and α_{VIII} (right) with all β -tubulin isotypes) with eribulin in equilibrium state during last 5 ns of MD simulations.

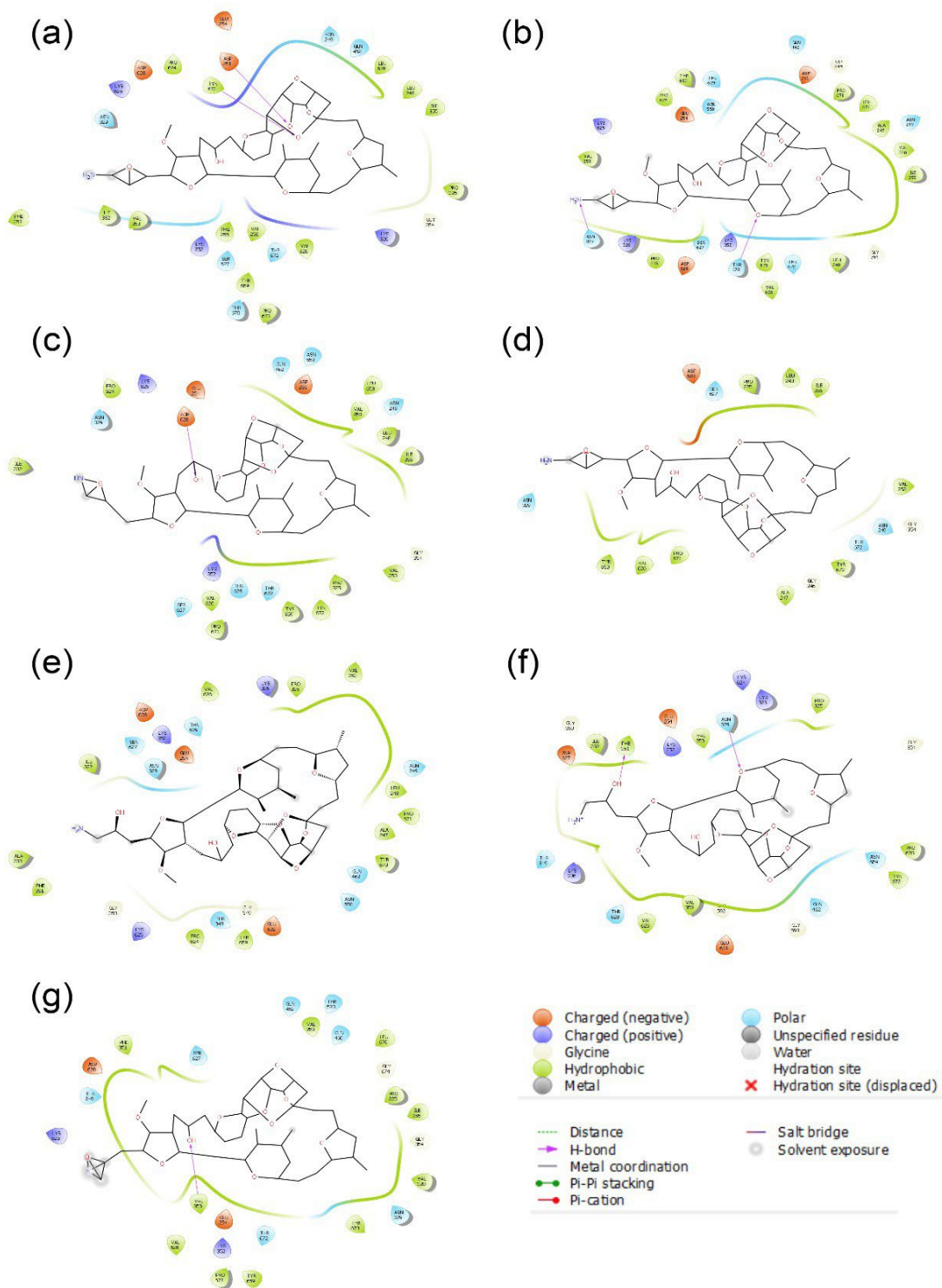


Fig. S7: 2D diagram of average interactions of eribulin during last 10 ns of MD simulation with combination of α_1 and (a) β_I , (b) β_{II} , (c) β_{III} , (d) β_{IV} , (e) β_{VI} , (f) β_{VII} , (g) β_{VIII} .

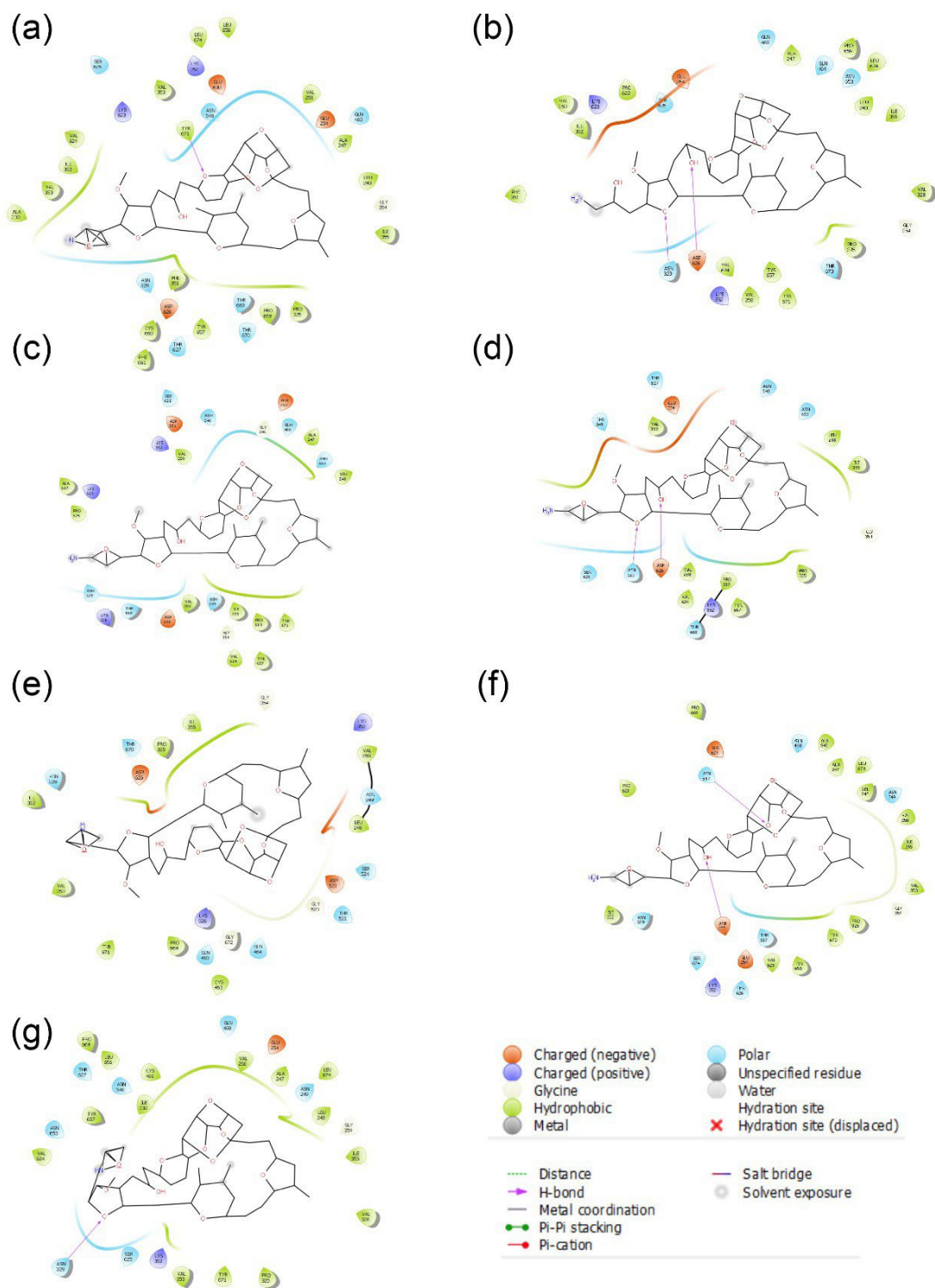


Fig. S8: 2D diagram of average interactions of eribulin during last 10 ns of MD simulation with combination of α_{VIII} and (a) β_I , (b) β_{II} , (c) β_{III} , (d) β_{IV} , (e) β_{VI} , (f) β_{VII} , (g) β_{VIII} .

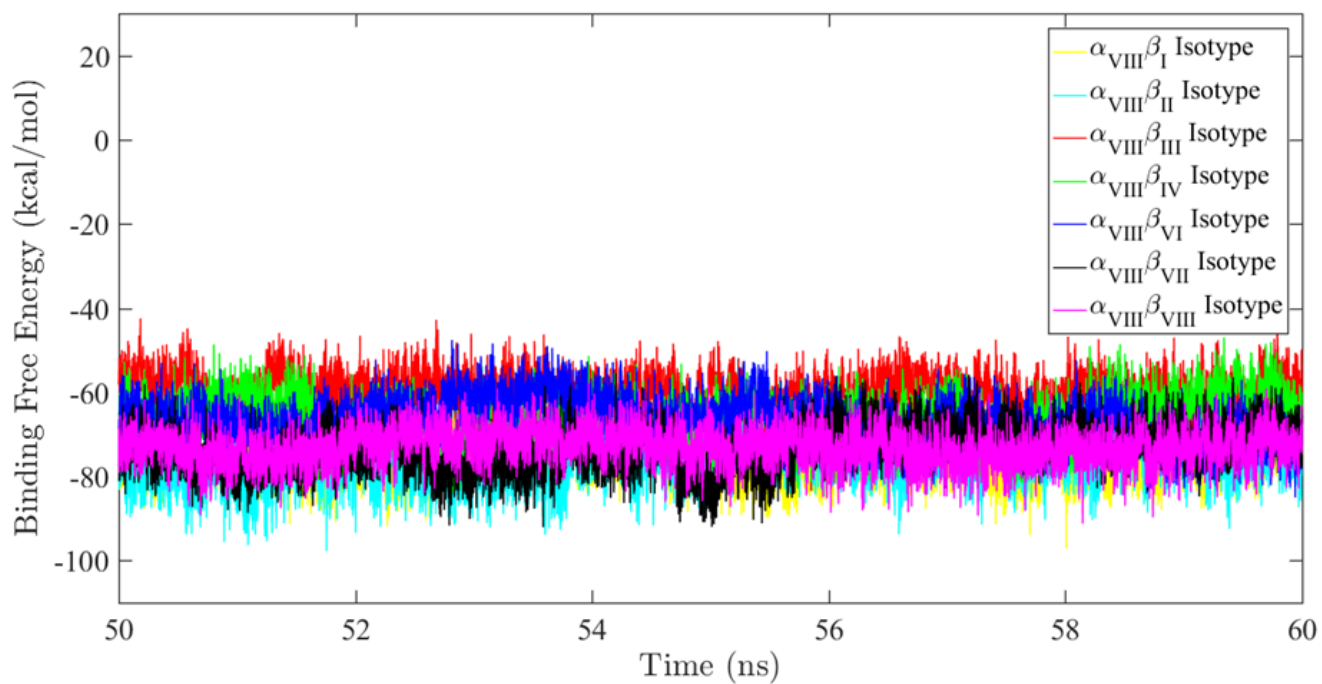
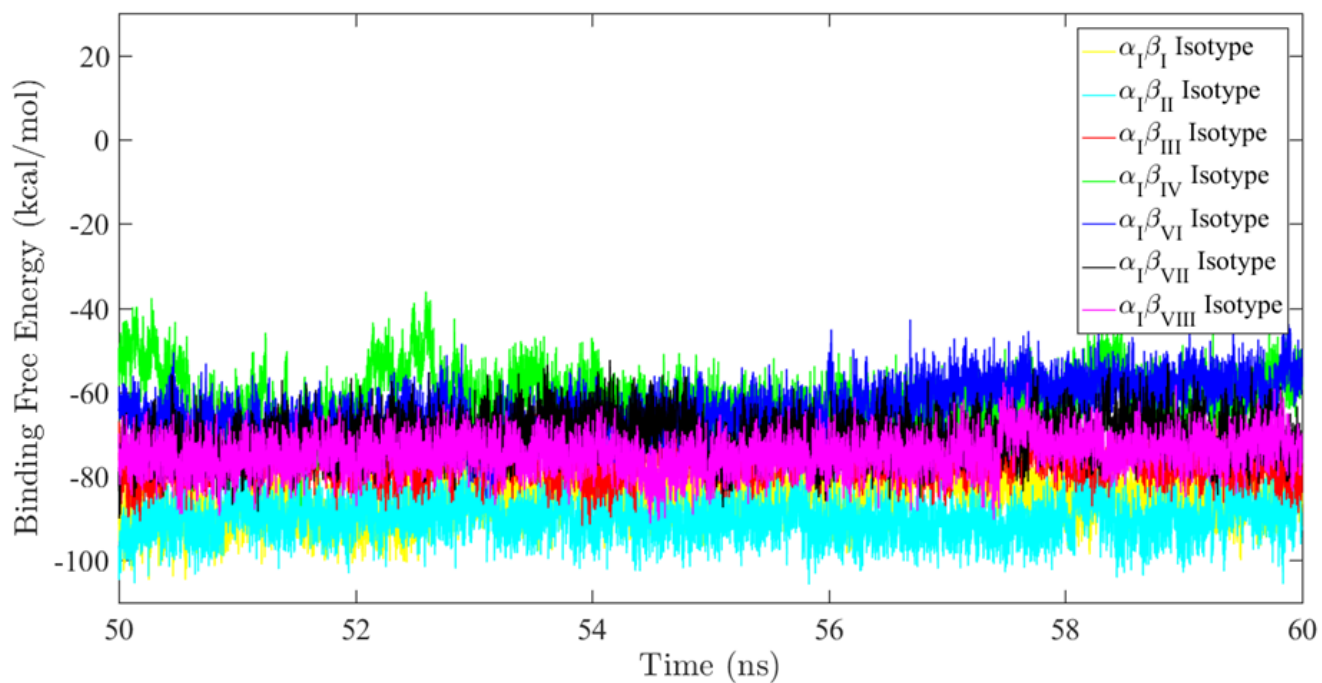


Fig. S9: Total binding free energy of tubulin isotypes with eribulin at equilibrium (during last 10 ns of MD simulations) for the combination of α I with 7 β tubulin isotypes (upper), and combination of α V III with 7 β .

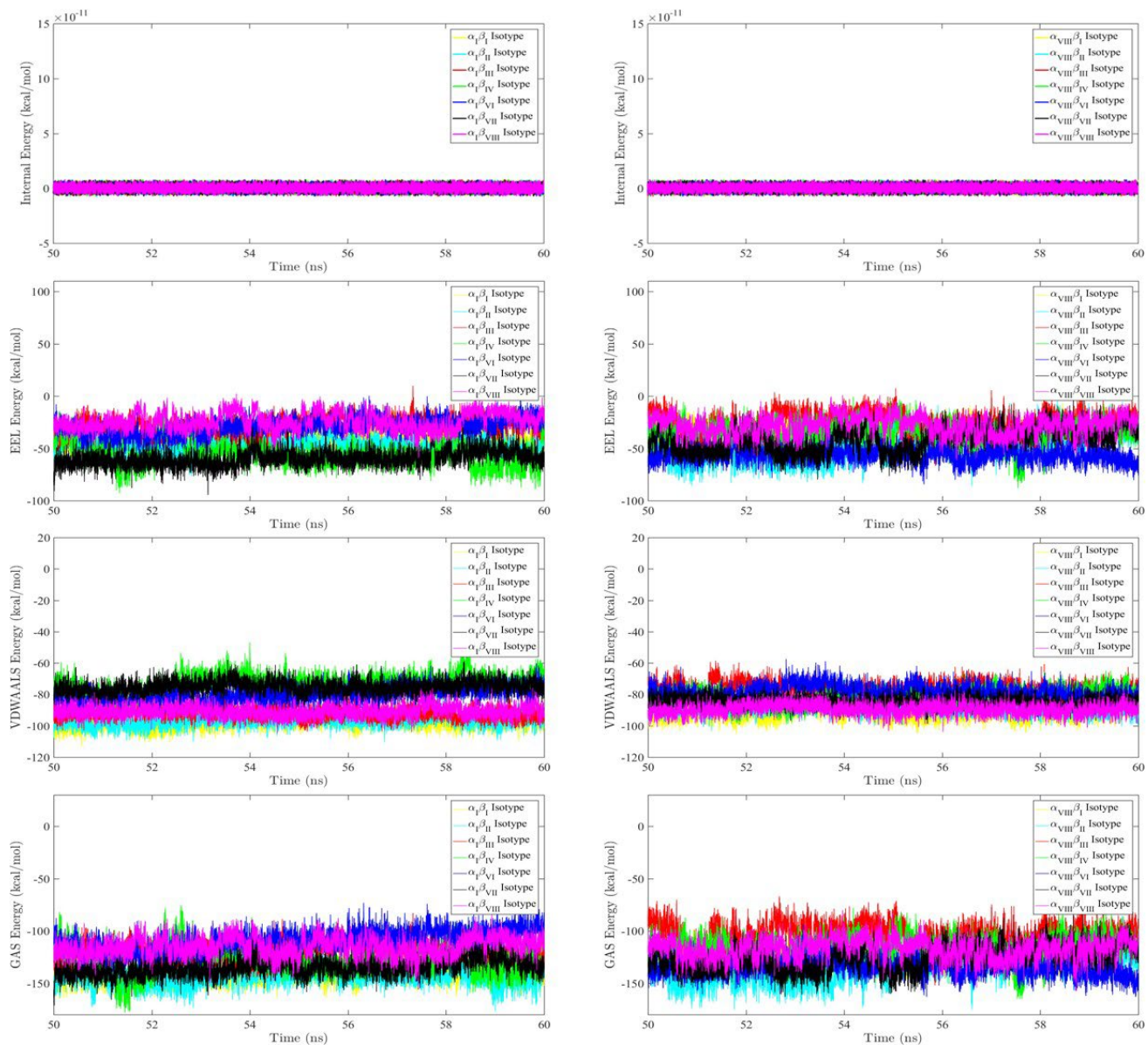


Fig. S10: Gas energy (lower) and its fractions internal (upper), electrostatic (upper middle), and van der Waal (lower middle) energies of all tubulin isotypes with eribulin in equilibrium state during last 10 ns of MD simulations (for α_I (left) and α_{VIII} (right) with all β -tubulin isotypes).

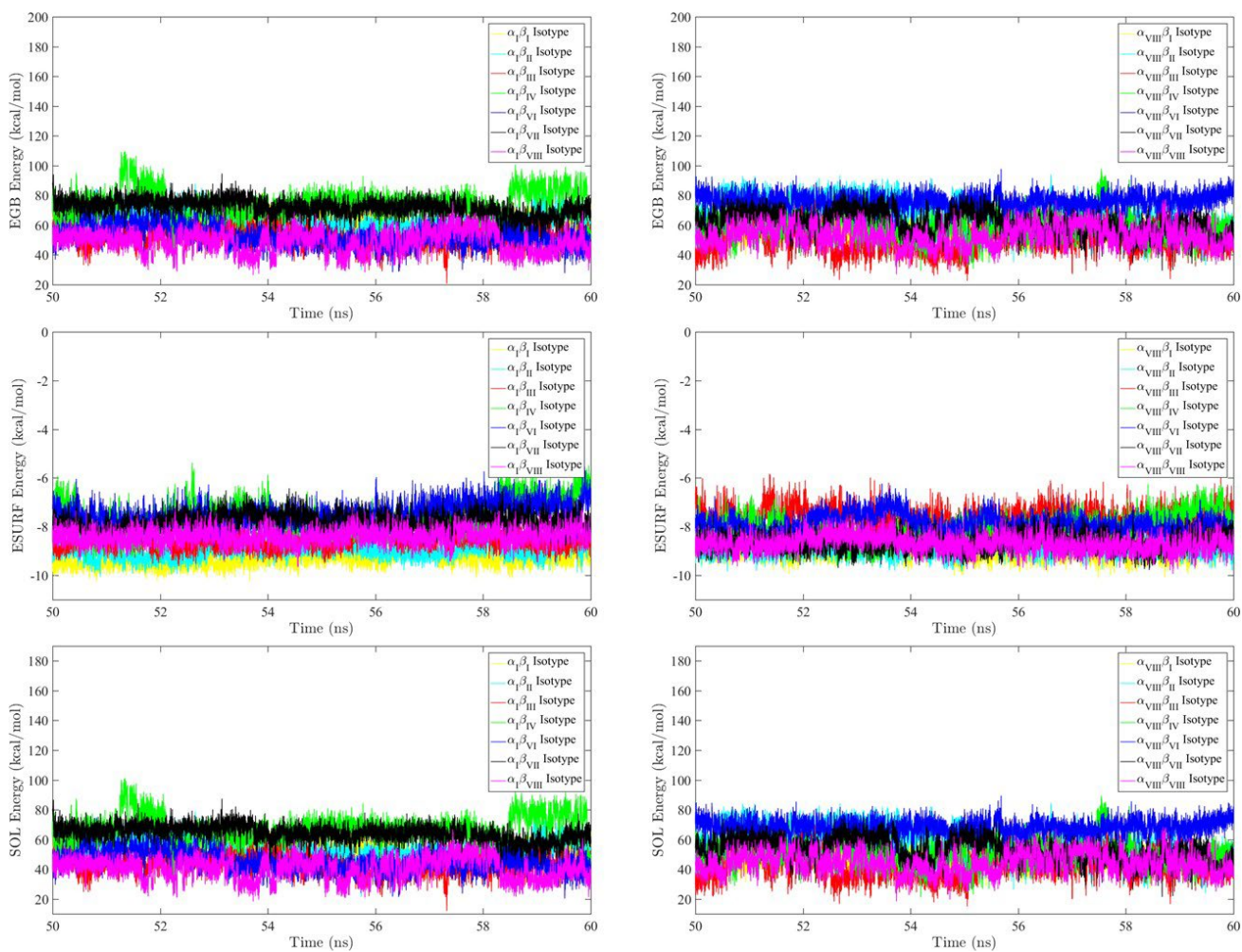


Fig. S11: Solvation energy (lower) and its fractions polar (EGB) (upper) and non-polar (ESURF) (middle) energies of all tubulin isotypes with eribulin in equilibrium state during last 5 ns of MD simulations.

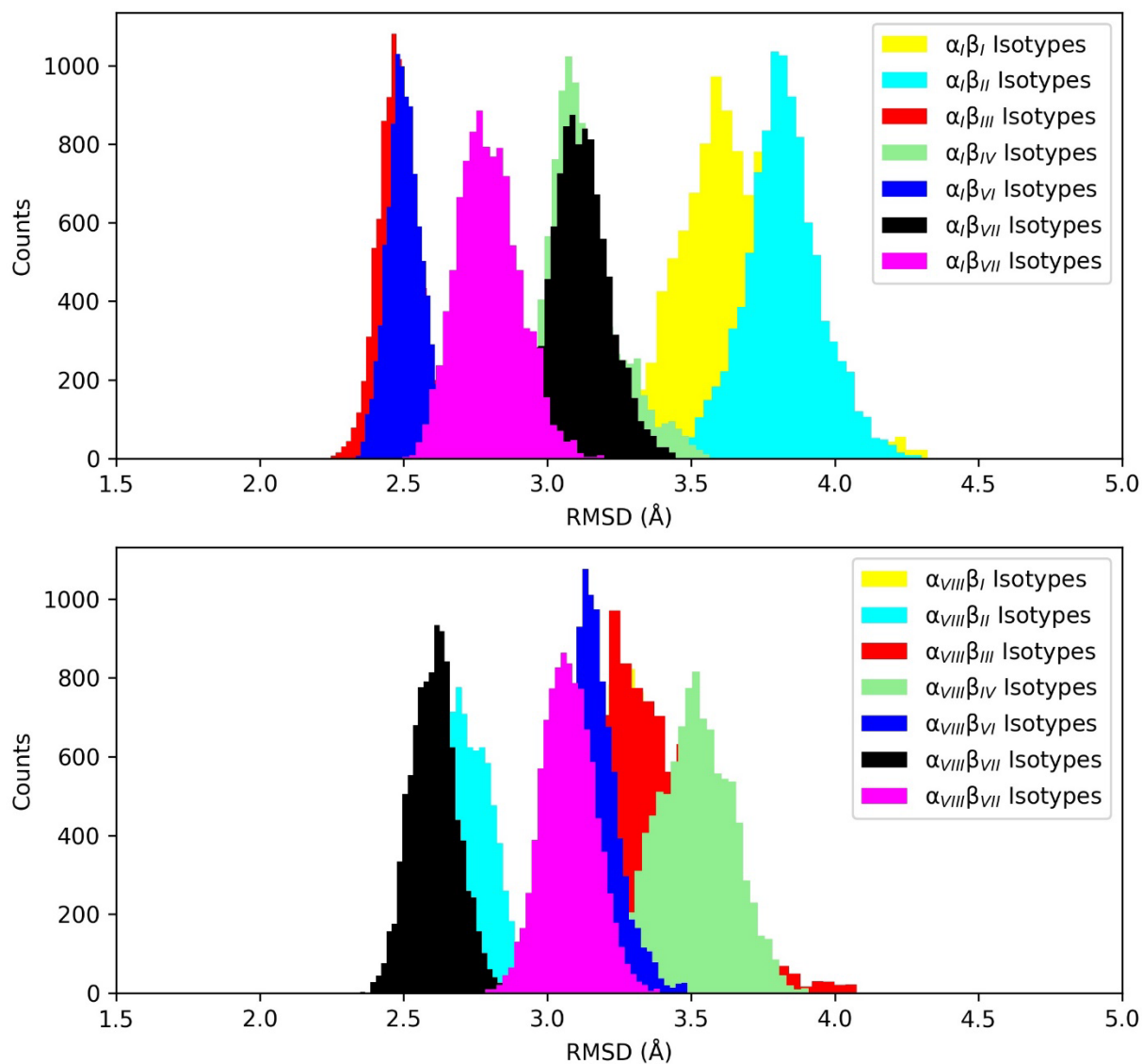


Fig. S12: Histograms of RMSD of backbone atoms during last 2 ns of MD simulations for combination of α_I with 7 β tubulin isotypes (upper), and combination of $\alpha_{V\ III}$ with 7 β tubulin isotypes (lower).

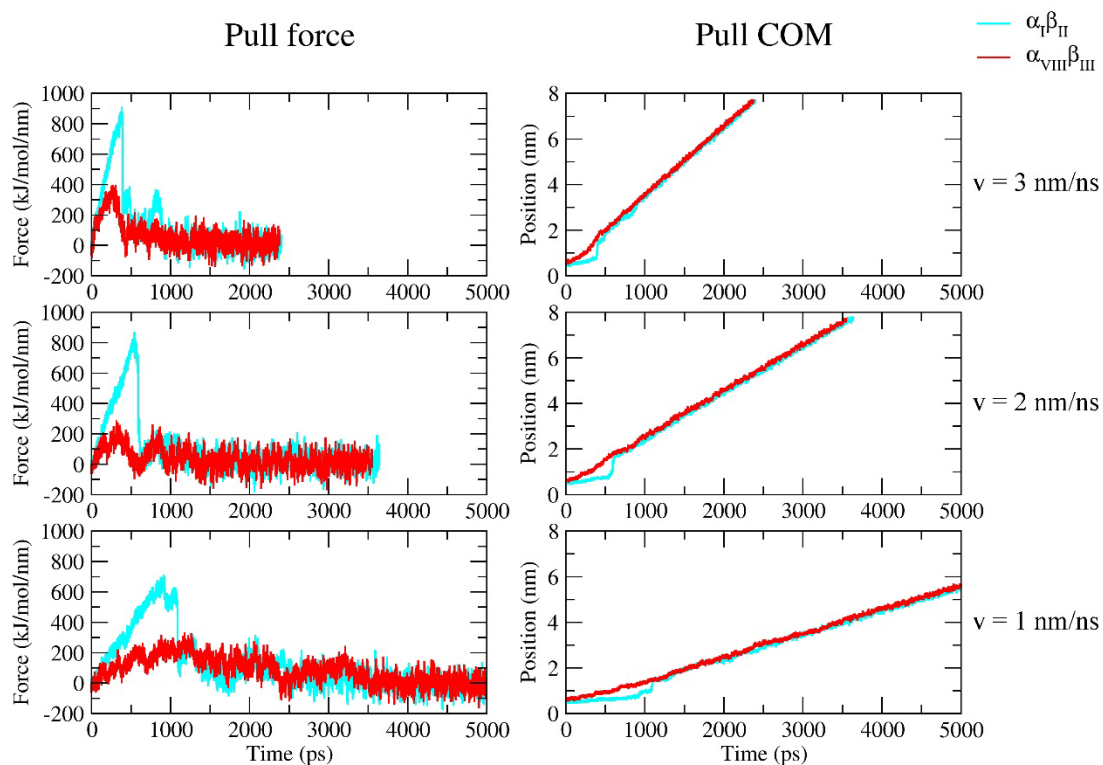


Fig. S13: Force and Displacement profiles obtained from steered molecular dynamics simulations starting with identical complex to explore the amount of force required to detach the eribulin from the $\alpha\beta_{II}$ and $\alpha_{VIII}\beta_{III}$ tubulin heterodimer with various velocities i.e. $v = 1$ nm/ns, $v = 2$ nm/ns, and $v = 3$ nm/ns.